4-10-1992

Paleomagnetism of the Middle Jurassic Summerville Formation, East Central Utah

David R. Bazard

Robert F. Butler
University of Portland, butler@up.edu

Follow this and additional works at: http://pilotscholars.up.edu/env_facpubs

Part of the Environmental Sciences Commons, and the Geophysics and Seismology Commons

Paleomagnetism of the Middle Jurassic Summerville Formation, East Central Utah

DAVID R. BAZARD[1] AND ROBERT F. BUTLER

Department of Geosciences, University of Arizona, Tucson

The paleomagnetism of the late Callovian(?) Summerville Formation was analyzed to obtain a late Middle Jurassic paleomagnetic pole for North America. A total of 281 samples were collected from 35 sedimentary horizons (sites) in a single locality in the San Rafael Swell area of east central Utah. Fifteen site-mean characteristic remanent magnetization (ChRM) directions pass the reversals test and define at least five polarity zones within 52 m of stratigraphic section, suggesting that the ChRM was acquired upon, or soon after, deposition. Magnetizations of some specimens are complex, and several horizons yield anomalous site-mean directions. Data analysis included filtering to provide different combinations of virtual geomagnetic poles for calculation of the paleomagnetic pole. However, editing the data did not change the pole position by more than 5°. The preferred paleomagnetic pole position is 56.3°N, 133.4°E ($A_{95} = 7.2°$; $N = 11$ sites). The Summerville Formation paleomagnetic pole is located near the ~172 Ma Corral Canyon pole and is statistically indistinguishable from the ~151 Ma Glance Conglomerate and ~149 Ma Lower Morrison poles. The paleomagnetic pole from the Summerville Formation is located at a much lower latitude and more easterly longitude than the paleomagnetic pole obtained from the ~165 Ma Moat Volcanics of New England. We propose that the Jurassic North American apparent polar wander path is an age-progressive band at 55°N to 65°N latitude extending from ~110°E longitude at ~172 Ma to ~150°E longitude at ~149 Ma.

INTRODUCTION

The geometry of the Jurassic apparent polar wander (APW) path for North America is controversial due to limited resolution of Jurassic paleomagnetic poles and conflicting results from similar age rocks. A better constrained Jurassic APW path appeared to result from addition of Jurassic paleomagnetic poles from Middle and Late Jurassic volcanic rocks [*Kluth et al.,* 1982; *May et al.,* 1986], exclusion of poorly defined paleomagnetic poles [*May and Butler,* 1986], and application of a paleomagnetic Euler pole (PEP) model for Jurassic APW [*Gordon et al.,* 1984]. However, recent studies have questioned the reliability of even the few Jurassic paleomagnetic poles selected for these latter compilations. Paleomagnetic poles from the Newark trend igneous intrusions [*Smith and Noltimier,* 1979], once thought to be "cornerstones" of the Jurassic APW path, are now questioned because of inadequate sampling of paleosecular variation [*Prevot and McWilliams,* 1989] and may be biased by a pervasive remagnetization [*Witte and Kent,* 1989, 1990]. Analyses of secondary magnetizations from Newark Basin sediments [*Witte and Kent,* 1989, 1990] and magnetizations from igneous rocks of New England [*Van Fossen and Kent,* 1990] have been interpreted to indicate a high-latitude Middle Jurassic APW path. This conflicts with paleomagnetic poles from Jurassic volcanic rocks of Corral Canyon [*May et al.,* 1986] and the Glance Conglomerate [*Kluth et al.,* 1982] in southeastern Arizona as well as poles predicted by the PEP model of *Gordon et al.* [1984].

Analysis of the Summerville Formation was undertaken to help resolve these conflicts. Specifically, a well-determined paleomagnetic pole from the ~158 Ma Summerville Formation would help distinguish between a Middle Jurassic APW path located at high latitudes as suggested by the paleomagnetic pole from the ~165 Ma Moat Volcanics [*Van Fossen and Kent,* 1990]

or a lower-latitude APW path suggested by the ~172 Ma Corral Canyon and ~151 Ma Glance Conglomerate paleomagnetic poles. Previously, *Steiner* [1978] found that a pervasive Cenozoic overprint magnetization allowed only 23 of her 391 paleomagnetic samples from the Summerville Formation to be used for determination of the paleomagnetic pole.

To resolve the characteristic remanent magnetization (ChRM) of the Summerville Formation, we collected multiple cores from numerous sedimentary layers (each sedimentary layer is considered a paleomagnetic site) and evaluated each using detailed thermal demagnetization (at least 11 steps up to the Curie temperature of hematite, ~680°C) and principal component analysis [*Kirschvink,* 1980]. These techniques allowed evaluation of within-site (within stratigraphic layer) dispersion of magnetization directions and identification of specimens and sites containing complex, multicomponent, magnetizations. The resulting data allowed objective rejection of sites and specimens with complex magnetizations in favor of sites and specimens with uniform, single-component ChRMs.

LOCATION, GEOLOGY, AND AGE

The Summerville Formation was sampled at three locations in eastern Utah and northeastern Arizona (Figure 1a). Preliminary data from these locations showed the coarser-grained Summerville Formation of southeastern Utah and northeastern Arizona (now assigned to the Wanakah Formation by *Condon and Huffman* [1988]) to retain either a late Cenozoic magnetization or complex, multicomponent magnetization. Yet, some of the finer-grained lithologies from the San Rafael Swell region of east central Utah appear to retain primary(?) magnetization. Therefore, further sampling was concentrated at the San Rafael Swell location (location 3 in Figure 1a).

The Summerville Formation at the San Rafael Swell location consists largely of thin-bedded, reddish-brown mudstone and siltstone with scattered thin beds of fine-grained, reddish-brown sandstone and minor lenses of gypsum. At this location the Summerville Formation lies gradationally above the marine Curtis Formation which in turn is separated from the underlying Entrada Sandstone by the J3 unconformity of *Pipiringos and O'Sullivan* [1978] (Figure 1b). The overlying Morrison Formation is separated from the Summerville Formation by the J5 unconformity of *Pipiringos and O'Sullivan* [1978]. The

---

[1]Now at Department of Geology and Geological Engineering, University of Mississippi, University.
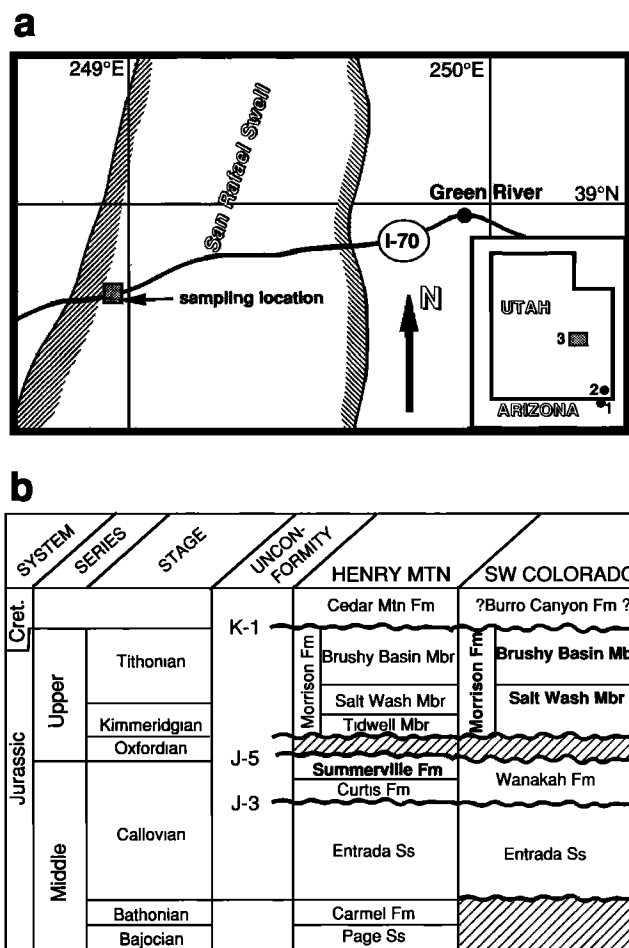
a

b

Fig. 1. Site location and stratigraphic context of the Summerville Formation. (a) Site location maps. Data presented in Table 1 are from location 3 (San Rafael Swell region, east central Utah: 38.84°N, 248.88°E). (b) Regional Middle and Late Jurassic stratigraphy of southeastern Utah and southwestern Colorado. Modified from *Baars et al.* [1988].

lithology and stratigraphy of the Summerville Formation suggest deposition in a shallow, restricted marine environment near the margin of the retreating Curtis sea in overbank, fluvial, and mudflat environments [*Baars et al.*, 1988]. The Summerville Formation at the sampling locality is essentially undeformed except for a shallow (3°) regional northwest dip associated with gentle folding of the San Rafael Swell above a Laramide basement-cored uplift.

No fossils have been found in the Summerville Formation of the San Rafael Swell region, but its age is constrained by the underlying Curtis Sandstone [*Imlay*, 1980], the overlying Morrison Formation [*Kowalis et al.*, 1991], and regional unconformities [*Pipiringos and O'Sullivan*, 1978] (Figure 1b). *Imlay* [1980] assigned a Callovian age to the Curtis Sandstone using a correlation between the Curtis Sandstone and the pre-early Oxfordian Pine Butte Member of the Sundance Formation in Wyoming as an upper age constraint, and a latest Bajocian age for the lowest limestone unit in the underlying Carmel Formation on the west side of the San Rafael Swell as a lower age constraint. *Pipiringos and O'Sullivan* [1978] showed that the Curtis Sandstone and conformably overlying Summerville Formation in the Uinta Mountains are separated from the underlying early to middle Callovian Entrada Sandstone by the J5 unconformity and separated from the overlying early to middle Oxfordian Redwater Shale Member of the Sundance Formation

by the J3 unconformity. These constraints bracket the age of the Summerville Formation as late Callovian to earliest Oxfordian (~160 Ma to ~156 Ma using the time scale of *Harland et al.* [1990]).

PALEOMAGNETIC RESULTS

Thirty-five sites (five to eight cores per site) covering approximately 52 m of stratigraphic section were sampled at the San Rafael Swell location (latitude 38.84°N, longitude 248.88°E, Figure 1a). Experimental procedures and laboratory equipment used to analyze the paleomagnetism of these samples are described by *Bazard and Butler* [1991]. Natural remanent magnetization (NRM) directions of specimens generally were either north or southeast directed with positive inclinations; magnetic intensities ranged from 5.8×10^{-4} A/m to 1.2×10^{-2} A/m. Thermal demagnetization of pilot specimens from each site (up to 18 temperature steps) revealed a few specimens which exhibit vector endpoint trajectories toward the origin of vector plots above 500°C (e.g., SV019F1, Figure 2a). However, many specimens are either overprinted by a component of magnetization directed along the present magnetic field direction or retain a ChRM which is determined only through thermal demagnetization at multiple steps between 650°C and 680°C (Figures 2b and 2c). To isolate this high unblocking-temperature ChRM, the remaining specimens were demagnetized using approximately four temperature steps between 200°C and 575°C and seven or more temperature steps between 600°C and 680°C.

Linear trends on vector component diagrams indicate isolation of a single, high unblocking-temperature ChRM for three or more specimens from 18 of the 35 sites (a total of 97 specimens). Specimen ChRM directions were obtained by fitting least squares lines [*Kirschvink*, 1980] to five or more thermal demagnetization steps between 595°C and 678°C and using the origin of vector diagrams as an additional equal-weighted data point. These ChRM directions were then used to calculate site-mean directions and associated Fisher statistics (Table 1). In addition, each site-mean direction listed in Table 1 has been corrected for the 3° NW regional dip. The other 17 sites were rejected from further consideration because (1) three or more of the eight samples at the site did not yield a single, high unblocking-temperature component of magnetization (as defined by a line-fit maximum angular deviation of <15°), or (2) within-site dispersion of specimen magnetization directions produced a site-mean with $\alpha_{95} > 25°$.

There is little correlation between lithology and the rejection of sites. Even the few coarser-grained lithologies include both acceptable (SV027) and rejected (SV017) sites. However, there may be a relationship between the presence of a single high unblocking-temperature ChRM and the site's proximity to a polarity zone boundary. Figure 3 shows many of the rejected sites are within ~2 m of a polarity zone boundary (e.g. SV015, SV026, SV036, SV012). Furthermore, the demagnetization of specimens from several of these sites produced curved vector component trajectories or unusual ChRM directions (unlike other Jurassic or Cenozoic directions reported for North America). This suggests these sites retain multiple high unblocking-temperature components that each record different polarity states (or transitional positions) of the magnetic field.

The instability and unusual directions obtained from the rejected sites also may be related to how the ChRM was acquired. Unfortunately, petrographic information concerning the magnetic mineralogy is typically obtained from coarser-grained lithologies. This information does not apply to the majority of sites of this study (which are fine grained) nor does it necessarily represent the minerals retaining the ChRM (even in the coarser-grained sites). Therefore we refer to the demagnetization data which show the ChRM for most sites is retained by high unblocking-temperature hematite. Additionally, curved
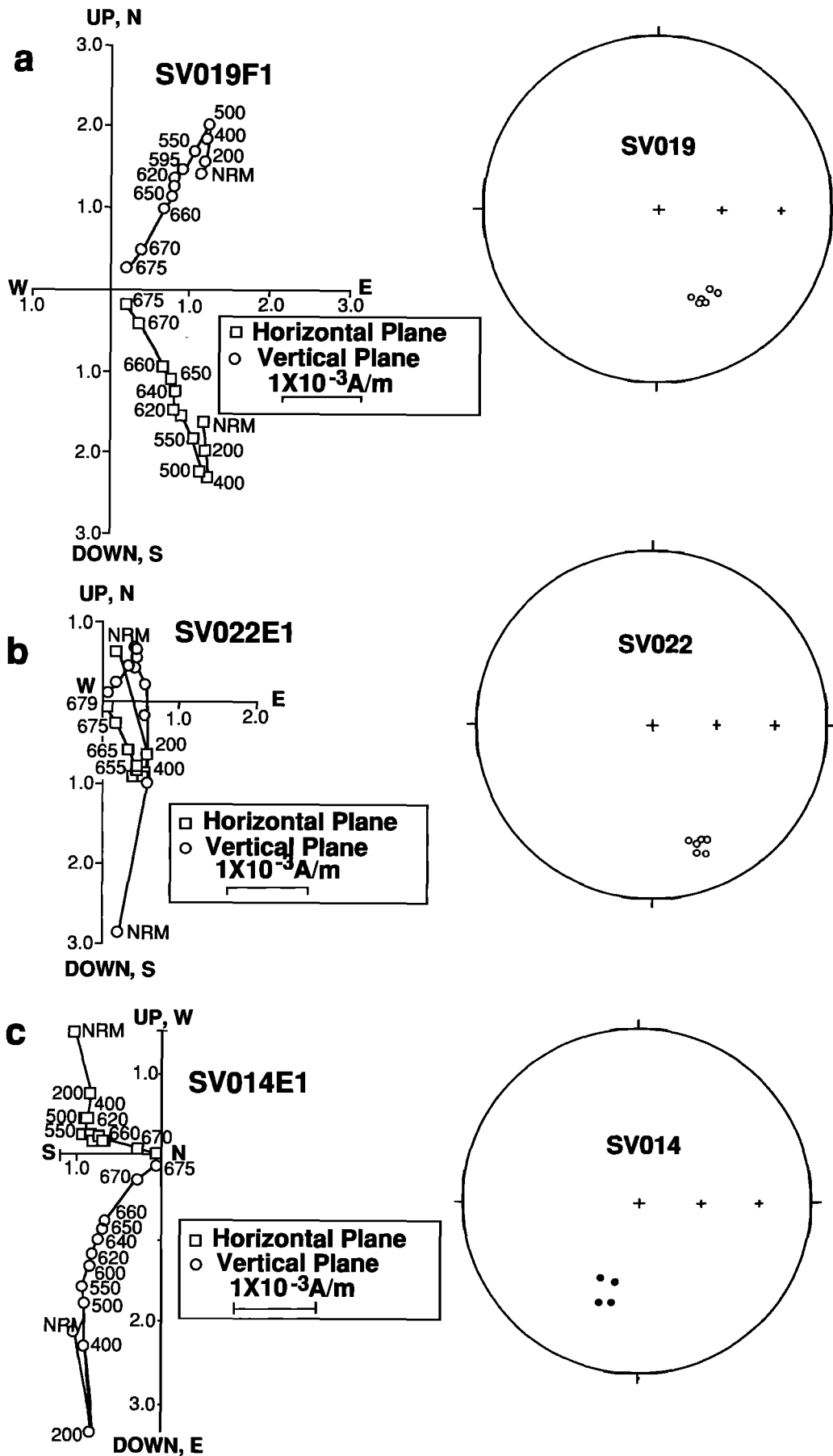
Fig. 2. Examples of the magnetization of the Summerville Formation. Vector endpoint diagrams are for individual specimens showing representative thermal demagnetization behavior. Equal-area projections show line fit directions for the highest unblocking-temperature component from each specimen within a site. Numbers adjacent to data points of the vector endpoint diagrams indicate thermal demagnetization temperatures in degrees Celsius. Open circles of equal-area projections are upper hemisphere; solid circles are lower hemisphere.

TABLE 1. Site-Mean ChRM Directions and Virtual Geomagnetic Poles

Site	N/N_O	T, °C	N_s	D, deg	I, deg	R	k	α_{95}, deg	Plat, °N	Plon, °E
SV010	7/7	600-675	8	346.0	34.6	6.83	35	10.3	66.8	104.3
SV010	4/7	600-675	8	337.9	34.2	3.96	70	11.1	62.3	118.8
SV013*	6/7	640-675	5	338.3	29.4	5.80	24	13.8	60.1	114.4
SV013*	4/7	640-675	5	333.6	33.4	3.94	52	12.9	59.2	124.4
SV014†	4/4	620-675	6	199.9	44.8	3.96	67	11.3	-22.1	229.6
SV019	6/6	595-678	8	152.1	-41.9	5.98	251	4.2	-62.2	315.2
SV020	3/6	620-678	7	137.1	-50.2	2.93	30	23.0	-54.3	339.6
SV022	6/6	640-678	6	158.5	-25.6	5.98	279	4.0	-58.3	291.6
SV023	5/6	635-670	5	321.9	43.3	4.91	42	11.9	55.3	147.4
SV023*	4/6	635-670	5	326.5	41.0	3.96	71	11.0	57.8	140.4
SV024†	6/6	620-673	8	320.5	32.7	5.75	20	15.5	49.8	138.7
SV025	3/6	620-673	8	321.2	40.3	2.96	48	18.1	53.4	144.7
SV027	6/8	640-673	6	125.6	-30.5	5.92	61	8.7	-37.7	329.4
SV027*	5/8	640-673	6	129.6	-30.9	4.97	157	6.1	-40.9	326.7
SV028†	5/6	620-678	9	112.9	-21.2	4.92	52	10.7	-24.7	333.1
SV029†	6/7	620-678	9	149.4	-7.4	5.90	52	9.4	-45.2	295.0
SV030†	8/8	620-678	9	149.4	-47.9	7.76	29	10.5	-62.9	326.8
SV032†	5/5	630-670	6	49.9	-5.1	4.93	60	10.0	28.3	8.7
SV033†	5/5	630-674	7	85.7	-10.5	4.95	74	8.9	0.1	345.7
SV040	6/6	620-678	9	164.4	-19.5	5.97	176	5.1	-58.0	278.8
SV042	5/6	620-678	9	153.9	-30.8	4.97	119	7.0	-58.2	301.9
SV043	5/5	620-673	8	129.8	-31.7	4.95	86	8.3	-41.4	327.1

N, number of specimens used to determine site-mean ChRM direction, virtual geomagnetic pole (VGP), and associated statistics; N_O, number of specimens thermally demagnetized; T, maximum thermal demagnetization temperature range over which principal component analysis was applied; N_s, maximum number of demagnetization steps within demagnetization temperature range; D, site-mean declination; I, site-mean inclination; R, length of resultant of N unit vectors; k, best estimate of Fisher precision parameter; α_{95}, radius of the cone of 95% confidence about the mean direction; Plat, latitude of site-mean VGP; Plon, longitude of site-mean VGP. All data corrected for 3° NW dip.

*Site recalculated from selected specimens (see text).

†Sites excluded from some paleomagnetic pole determinations (see text and Table 2).

demagnetization trajectories of some specimens and the high within-site dispersion of rejected sites may be due to protracted, or multiple periods of, hematite growth. We suspect that during periods of constant polarity the specimens average secular variation and retain a reliable record of the dipolar geomagnetic field. However, during polarity transitions or excursions the specimens of a site record several directions, and thus these specimens retain multiple high unblocking-temperature components. Alternatively, the specimens from a single site may each record a different direction; this would result in a large within-site dispersion.

Virtual geomagnetic poles (VGPs) calculated from the 18 accepted sites are listed in Table 1 and plotted in Figure 4a. Reversed-polarity (southern hemisphere) VGPs have been inverted to the northern hemisphere. These VGPs and associated site-mean directions define at least five polarity zones within the 52 m of stratigraphic section (Figure 3). However, many layers consisting of coarse-grained or poorly consolidated material were not sampled. Thus the stratigraphic extent and number of polarity zones within this section are not complete. Nevertheless, the observed polarity zones argue for mixed polarity during the late Callovian–early Oxfordian interval of deposition.

A paleomagnetic pole and its associated 95% confidence region were calculated from the 18 VGPs and are shown in Figure 4a and listed in Table 2 (pass A). The large confidence region ($A_{95} = 14.5°$) is due primarily to three outlying VGPs from sites SV014, SV032, and SV033. Each of these VGPs are over two angular standard deviations ($2\delta = 61.2°$) from the mean of all 18 VGPs. There is no obvious aspect of vector endpoint diagrams (e.g., Figure 2c), within-site dispersion, or structural setting indicating the cause of these aberrant site-mean directions. However, each of these sites is within 3 m of a polarity zone boundary, suggesting that the magnetization during polarity transition or mixing of normal- and reversed-polarity compo-

nents of magnetization accounts for their aberrant directions. Because these sites are not representative of the VGP distribution, a second paleomagnetic pole was calculated after excluding VGPs from these three sites. The remaining 15 VGPs and the resulting paleomagnetic pole and associated confidence region are shown in Figure 4b. The paleomagnetic pole and associated statistics are listed as pass B in Table 2. Exclusion of the three aberrant VGPs changes the paleomagnetic pole position by about 4° (angle between the two poles listed in Table 2) and substantially reduces the dispersion of the VGPs (K changes from 6.6 to 25.9) and the confidence region (A_{95} decreases from 14.5° to 7.7°).

A third pass at calculating a paleomagnetic pole was performed after evaluating within-site dispersion. Collecting multiple samples per site allowed identification of anomalous specimen ChRM directions and aberrant within-site distributions. Therefore, for the third pass (pass C), specimens with ChRM directions anomalous to the majority of specimens from a site (e.g., Figure 5a) were rejected and the site-mean direction and corresponding VGP were recalculated (marked by asterisks in Table 1). In addition, VGPs obtained from four sites exhibiting streaking of specimen directions (e.g., Figure 5b) were excluded. Sites excluded for the pass C calculation of the paleomagnetic pole are indicated by daggers in Table 1. The remaining 11 VGPs (obtained from 51 specimens) of pass C are shown in Figure 4c along with the resulting paleomagnetic pole and confidence region (Table 2). These data also are listed as pass C in Table 2. Although pass C involves a substantial amount of data editing, the resulting paleomagnetic pole and confidence interval are similar to those resulting from pass B.

Similar paleomagnetic pole positions were obtained using these different data selection criteria (Table 2). The most dramatic change resulted from exclusion of the three sites in pass A (compare pass A and pass B, Table 2). The VGP distributions of passes B and C are Fisherian at the 95% confidence level (using

the chi-square test of *McFadden* [1980]), whereas the distribution of pass A is not. Nevertheless, the means of the normal- and reverse-polarity site-mean directions are statistically indistinguishable from antipodal (at the 95% and 99% confidence level) for each pass. However, as shown by *McFadden and McElhinny* [1990], a positive reversals test may indicate lack

of information rather than well-determined, antipodal directional distributions. The site-mean directional distribution of pass A falls into such an "indeterminate" category (Ri of *McFadden and McElhinny* [1990]). Although the means of the normal- and (inverted) reverse-polarity distributions of pass A are statistically indistinguishable at the 95% confidence level, they are separated by an angular distance of 18.3° and would be statistically indistinguishable even if separated by greater than 20°. Thus the positive reversals test for the pass A data is the result of large directional dispersion and cannot be used to argue for lack of systematic secondary components nor early acquisition of ChRM.

In contrast, the normal- and (inverted) reverse-polarity directional distributions of passes B and C are less dispersed and the means are separated by less than 7° (6.4° for pass B and 3.7° for pass C). According to the procedure of *McFadden and McElhinny* [1990] these directional distributions yield a C classification reversals test (Rc). That is, the mean directions for each polarity group must be separated by 10° to 20° before they fail the reversals test at the 95% confidence level (pass B fails at 16.5°, and pass C fails at 13.8°). Although an "A" classification (polarity group means fail when separated by >5°) is desirable, *McFadden and McElhinny* [1990] showed that out of 535 reversals tests from a global paleomagnetic data base, only seven satisfy the criteria for class A passage of the reversals test and 48 pass as class B (polarity group means fail when separated by >10°). Moreover, most reversals tests were classified as indeterminate. Thus the reversals tests for passes B and C of the Summerville Formation data are typical of most positive reversals tests where sufficient information is available to evaluate the quality of the test. We use these positive reversals tests, the existence of at least five polarity zones, and the proximity of rejected sites to polarity boundaries as evidence that the high unblocking-temperature ChRM was acquired within the first few 10^5 years after late Callovian deposition. Thus many rejected sites are interpreted as acquiring multiple ChRMs during periods of mixed polarity, while accepted sites are interpreted as acquiring single ChRMs during periods of constant polarity.

Paleomagnetic pole positions corrected for 4° of clockwise rotation of the Colorado Plateau are given in parentheses in Table 2. Although the amount (or existence) of Colorado Plateau rotation has been controversial, most geologic and paleomagnetic analyses suggest that post-Middle Jurassic rotation is limited to ≤6° [*Bryan and Gordon*, 1990; *Bazard and Butler*, 1991; *Hamilton*, 1981]. Another complication is the possibility of inclination shallowing of the ChRM direction due to sediment compaction as possibly suggested by the sites exhibiting within-site streaking toward shallower inclinations (Figure 5a). These sites were excluded from the pass C data set
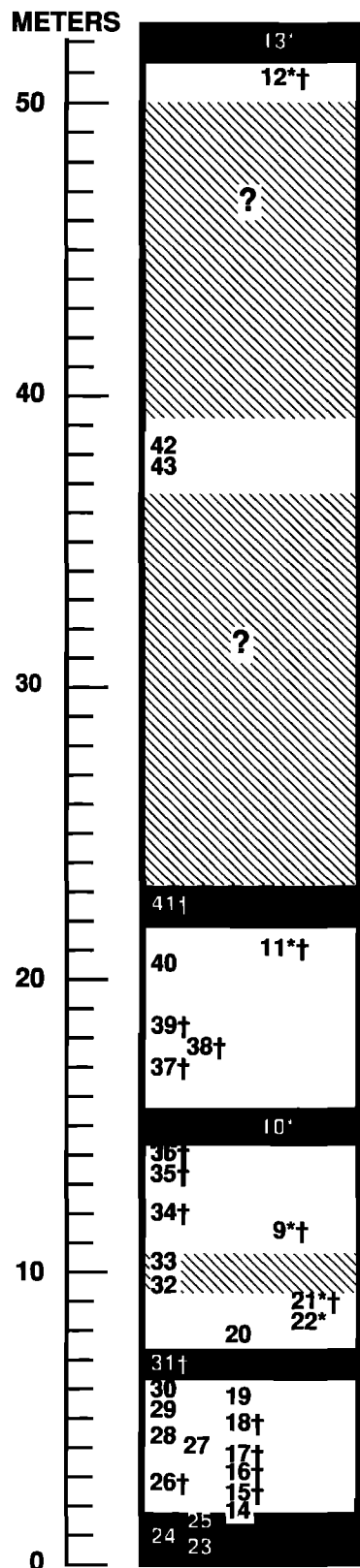

Fig. 3. Relative stratigraphic positions of sites and interpretations of the magnetic polarity of their ChRM. Each number corresponds to a paleomagnetic site. Solid regions are interpreted as normal polarity, and white regions are interpreted as reverse polarity. The diagonal lines represent sections where the polarity is unknown. Sites 9–13, indicated by asterisks, were destroyed during road construction (prior to sampling of sites 14–43); the correlation between these and other sites is questionable. Sites 21 and 22 (also indicated by asterisks) are located in a canyon adjacent to the main sampling area; the correlation of these sites relative to the other sites also is questionable. Sites with the superscript dagger were rejected from pole calculations (see text). In most cases the polarity of the ChRM from these sites was evident or at least consistent with our interpretations of adjacent sites. However, the polarity zones interpreted entirely from rejected sites (the normal-polarity zones defined by 31 and 41) should be considered tenuous. Therefore we propose only five different polarity zones within the 52 m.
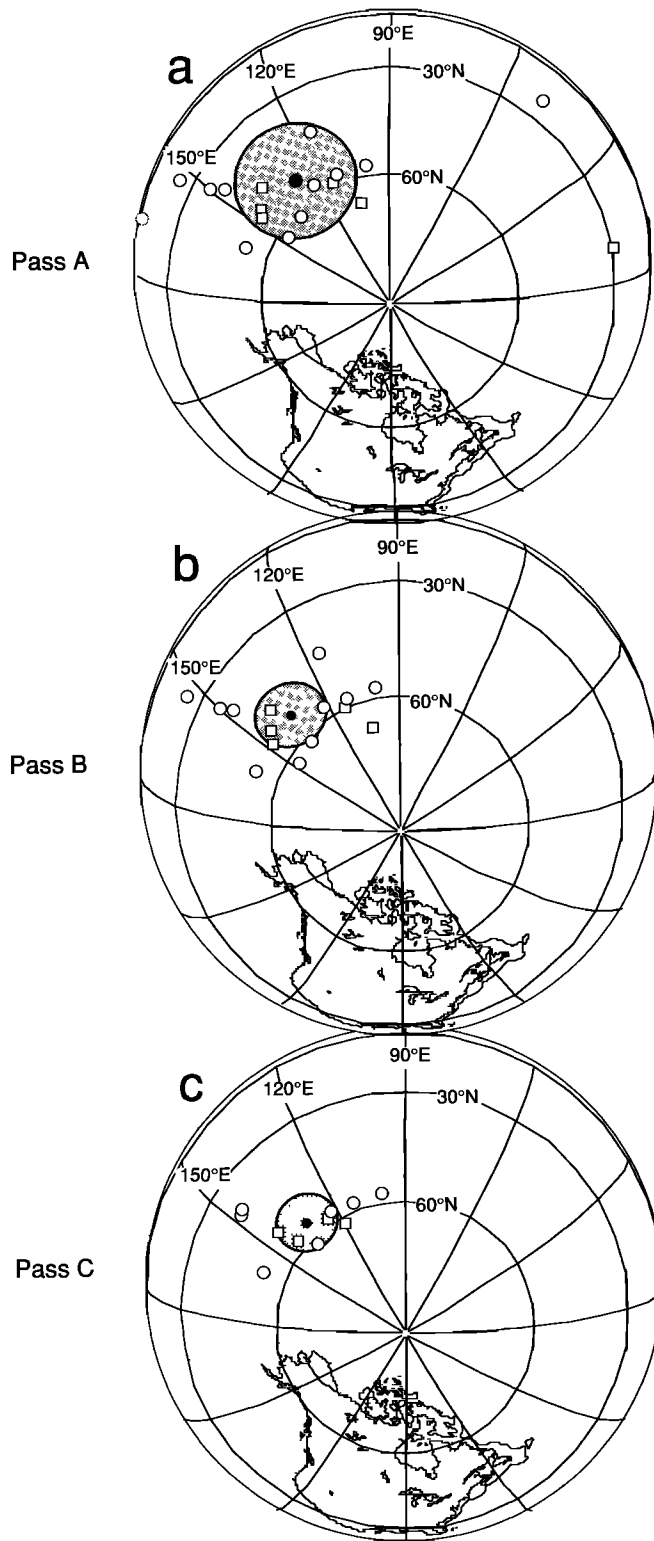
Fig. 4. Site-mean virtual geomagnetic poles (VGPs) and paleomagnetic poles for the Summerville Formation. (a) Pass A: 18 VGPs; all sites retaining a high unblocking-temperature ChRM. (b) Pass B: 15 VGPs; sites SV014, SV032, and SV033 excluded. (c) Pass C: 11 VGPs; sites exhibiting within-site streaking excluded; site-mean VGPs of four sites with anomalous specimens have been recalculated (marked by asterisks in Table 1). See Tables 1 and 2 for data listings and statistics. Squares are normal-polarity VGPs; circles are inverted reverse-polarity VGPs. Paleomagnetic poles are solid circles surrounded by shaded 95% confidence regions.

which provides the best estimate of the late Callovian paleomagnetic pole. Additionally, if the magnetization is the result of postdepositional chemical magnetization associated with cementation, then compaction shallowing of inclination may not be a concern. However, the relatively large dispersion of VGPs is not consistent with within-site and within-sample averaging of paleosecular variation as might be expected from chemical magnetization which occurred over several thousand years. Thus we cannot entirely dismiss the possibility of some inclination shallowing.

DISCUSSION AND CONCLUSIONS

Due to the problems discussed above, we favor the paleomagnetic pole positions obtained from the directional data sets of passes B and C. Because these poles are similar, the choice of which to use is somewhat arbitrary. We believe the paleomagnetic pole from pass C (11 VGPs, 51 specimens) is the most reliable because we feel the additional data selection is justified, especially if compaction shallowing of inclination contributes to the within-site streaking of the excluded sites. However, both the paleomagnetic poles of passes B and C suggest a similar APW path geometry, and both are considered in the following discussion.

Using the test of McFadden and Lowes [1981], the paleomagnetic poles determined from Summerville Formation directional data sets of passes B and C are statistically distinguishable from the older Corral Canyon pole (CC in Figure 6) at the 95% confidence level. However, both of these Summerville Formation paleomagnetic poles are statistically indistinguishable from the younger Glance Conglomerate and Lower Morrison Formation poles (GC and LM in Figure 6). Thus the ~158 Ma Summerville paleomagnetic pole (determined by either pass B or pass C) is consistent with an APW path segment determined by the ~172 Ma Corral Canyon , ~151 Ma Glance Conglomerate, and ~149 Ma Lower Morrison poles.

However, the Summerville Formation paleomagnetic poles determined from passes B and C are both statistically distinct from the Summerville Formation paleomagnetic pole determined by Steiner [1978]. In part, this may be because of data selected. For example, a Summerville pole determined by Steiner [1978] from 29 specimens is statistically indistinguishable from the paleomagnetic pole determined from our passes B and C, yet the poles preferred by Steiner [1978] based on 23 and 15 specimens are distinguishable from the paleomagnetic poles of passes B and C. These differences also may be due to the analysis methods used for each study. Steiner collected only one sample from each stratigraphic layer (her 22 to 45 cm spacing is greater than the thickness of most strata of this formation), and thus she was not able to evaluate within-layer (within-site) dispersion. We have found evaluation of within-layer dispersion of magnetization directions useful for identifying specimens and sites containing complex, multicomponent magnetizations. Additionally, we used detailed thermal demagnetization (in steps as small as 5°C) and principal component analysis to isolate the ChRMs (e.g., Figure 2b). In contrast, Steiner [1978] used demagnetization increments of ≥30°C and the Kirschvink [1980] method of principal component analysis was not available at the time of Steiner's analysis. Therefore, because these two Summerville Formation data sets have been obtained using substantially different methods, we did not combine the data sets to obtain a single pole. Instead, we present the pass B and pass C poles as the best representations of the late Callovian Summerville paleomagnetic pole.

The Summerville paleomagnetic poles of passes B and C are also statistically distinct from the 160 Ma paleomagnetic pole predicted from the PEP model of Gordon et al. [1984]. Although their 160 Ma pole is located close to our Summerville pole, we believe that inclusion of limited-resolution Jurassic poles

TABLE 2. Formation Mean ChRM Directions and Paleomagnetic Poles

		Mean Direction					Mean of VGPs				
	N	D, deg	I, deg	R	k	α_{95}, deg	Plat, °N	Plon, °E	R	K	A_{95}, deg
					Pass A (18 Sites)						
All	18	314.2	36.0	15.12	5.9	15.6	54.4 (51.9	127.6 132.6)	15.43	6.6	14.5
Normal	6	321.1	45.7	5.08	5.4	31.7	64.3	113.3	5.15	5.9	30.1
Reverse	12	131.4	−31.0	10.18	6.1	19.2	−49.1	312.3	10.45	7.1	17.5
				Pass B (15 Sites; Excludes SV014, SV032, and SV033)							
All	15	325.6	33.4	14.38	22.7	8.2	54.0 (51.2	134.8 139.3)	14.46	25.9	7.7
Normal	5	329.9	36.5	4.92	53.3	10.6	58.1	132.4	4.92	47.7	11.2
Reverse	10	143.5	−31.7	9.48	17.4	11.9	−51.9	315.9	9.56	20.7	10.9
			Pass C (11 Sites; Uses Asterisked Sites and Excludes Daggered Sites of Table 1)								
All	11	328.2	35.0	10.74	38.9	7.4	56.3 (53.6	133.4 138.2)	10.76	41.5	7.2
Normal	4	330.1	37.4	3.98	130.0	8.1	58.6	132.9	3.97	118.3	8.5
Reverse	7	147.1	−33.6	6.77	26.5	11.9	−54.9	313.7	6.79	28.5	11.5

N, number of sites; D, mean declination; I, mean inclination; R, length of N resultant unit vectors; k, best estimate of Fisher precision parameter of directional distribution; α_{95}, radius of cone of 95% confidence about direction; Plat, latitude of paleomagnetic pole; Plon, longitude of paleomagnetic pole; K, best estimate of Fisher precision parameter of VGP distribution; A_{95}, radius of cone of 95% confidence about paleomagnetic pole. Normal and reverse indicate polarity of subdivisions of data sets. Latitudes and longitudes in parentheses are paleomagnetic poles corrected for proposed 4° clockwise rotation of the Colorado Plateau. All data corrected for 3° NW dip. See text for selection criteria.
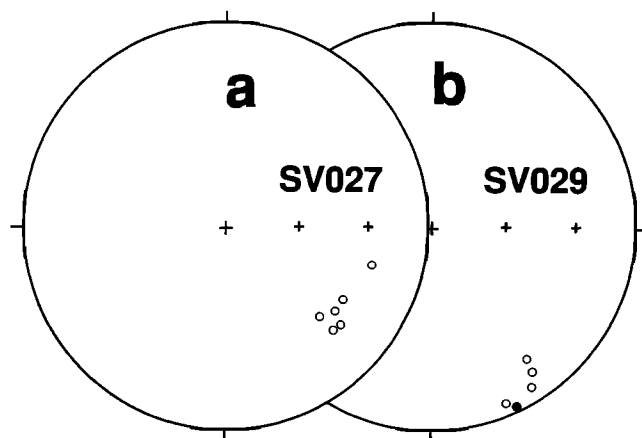

Fig. 5. Examples of sites or specimens excluded for pass C. (a) An example of a within-site distribution with one anomalous specimen direction. Such specimens were excluded to calculate the site-mean directions used for Pass C (marked by asterisks in Table 1). (b) Example of a streaked within-site distribution of specimen directions. Four sites (SV024, SV028, SV029, and SV030) were rejected from pass C using these criteria. Open circles are upper-hemisphere projections; solid circles are lower-hemisphere projections.

(including the previous Summerville pole) in their PEP analysis produced a bias of the 160 Ma pole toward higher latitudes.

More problematic is the paleomagnetic pole from the Moat Volcanics (MV in Figure 6 [Van Fossen and Kent, 1990]), which is inconsistent with all Middle and Late Jurassic poles from the red sedimentary rocks of the Colorado Plateau and volcanic rocks of southeastern Arizona. Although the Moat Volcanics

pole is consistent with paleomagnetic poles obtained from secondary components of magnetization in Newark Basin sedimentary rocks [Witte and Kent, 1989, 1990], neither the age nor the structural orientation during acquisition of these secondary components is known. A failed tilt test clearly shows a secondary origin of magnetization for the Moat Volcanics, and structural complication is evident given that the Moat Volcanics samples come from the interior of a collapsed caldera. Van Fossen and Kent argue that the Moat Volcanics ChRM was acquired soon after caldera collapse; however, there is no direct evidence to link the magnetization age with the ~165 Ma Conway granite as they suggest. We interpret the discrepancy between the position of the Moat Volcanics pole and the positions of Corral Canyon, Summerville, Glance Conglomerate, and Lower Morrison poles as the result of either late Tertiary remagnetization of the Moat Volcanics and/or postmagnetization structural complications.

Another approach to evaluating the geometry of the late Mesozoic North American APW path is to compare paleomagnetic poles from several plates by rotating these poles into a common reference frame. Because reconstructions of the Atlantic-bordering continents are well constrained for the Middle to Late Jurassic, such comparisons should reflect the quality of the paleomagnetic poles being compared rather than uncertainties in plate reconstructions. Using such a comparison, Van Fossen and Kent [1990] argued that the high-latitude position of the Moat Volcanics paleomagnetic pole is consistent with Jurassic poles of Europe and Gondwana. In contrast, Halvorsen [1989] showed that some European Jurassic paleomagnetic poles agree with the APW path as defined by the Middle and Late Jurassic poles from the southwestern United States [e.g., Heller, 1977; Kadzialko-Hofmokl et al., 1988], while other European poles occur at high latitudes and do not agree with the poles from the southwestern United States [e.g.,

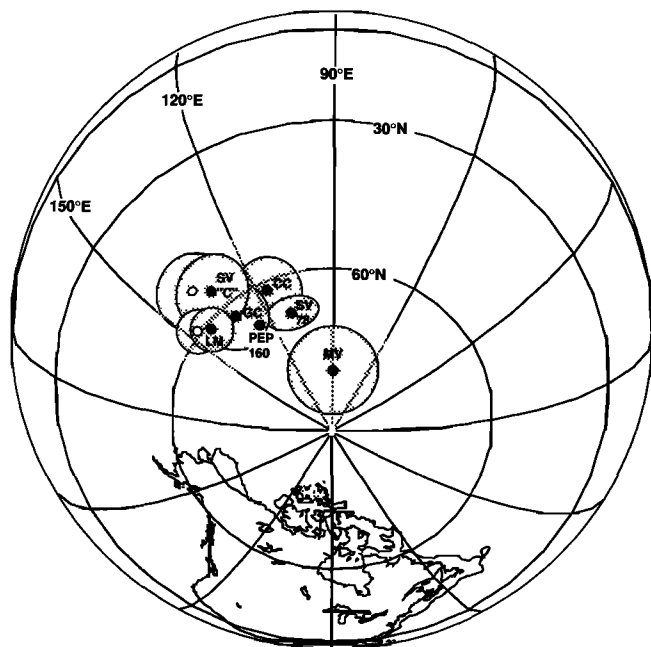BAZARD AND BUTLER: PALEOMAGNETISM OF SUMMERVILLE FORMATION, UTAH

Fig. 6. Comparison of Summerville Formation paleomagnetic poles to other Middle and Late Jurassic poles from North America. SV"C", Summerville paleomagnetic pole, 156–160 Ma, derived from 11 VGPs listed in Table 1 (pole and statistics listed as pass C in Table 2). SV78, Summerville Formation paleomagnetic pole calculated from 23 specimens [*Steiner*, 1978]. CC, Corral Canyon paleomagnetic pole, 172 ± 5.8 Ma [*May et al.*, 1986]. MV, Moat Volcanics paleomagnetic pole, 163–168 Ma (?) [*Van Fossen and Kent*, 1990]. PEP 160, 160 Ma paleomagnetic Euler pole model pole [*Gordon et al.*, 1984]. GC, Glance Conglomerate paleomagnetic pole, 151 ± 2 Ma [*Kluth et al.*, 1982]. LM, Lower Morrison paleomagnetic pole, 149 Ma(?) [*Steiner and Helsley*, 1975]. Paleomagnetic poles are solid circles surrounded by shaded 95% confidence limits. The open circles and surrounding confidence limits (lighter shading) are the Summerville paleomagnetic pole C and the Lower Morrison paleomagnetic pole corrected for 4° clockwise rotation of the Colorado Plateau.

Johnson et al., 1984; *Kadzialko-Hofmokl and Kruczyk*, 1987]. Moreover, *Halvorsen* [1989] noted that this latter group of European paleomagnetic poles were obtained from rocks with prefolding magnetizations. But because the folding is believed to be associated with Alpine orogenesis, the magnetizations could be as young as Miocene. This could explain the high latitudes of some of the Middle to Late Jurassic European paleomagnetic poles.

For Africa (and other Gondwana continents), very few reliable paleomagnetic poles are available. For example, *Besse and Courtillot* [1991] list only one African pole [*McElhinny and Jones*, 1965] for the 145–175 Ma period which passes their selection criteria. This pole falls at a high latitude (~74°N) in North American coordinates but has a confidence region (12°) which overlaps those of the Corral Canyon and Glance Conglomerate poles as well as the confidence region surrounding the paleomagnetic pole from the Moat Volcanics. Because of these complications, the Jurassic European and Gondwana poles do not provide the resolution required to distinguish between the alternative North American APW path geometries.

We prefer to determine the Jurassic North American APW path from the best available paleomagnetic poles from North America. The position of the paleomagnetic poles determined from the Summerville Formation is consistent with the APW segment described by the Corral Canyon and Glance Conglomerate poles. These three paleomagnetic poles are based on investigations which utilized detailed demagnetization

to isolate a ChRM. In each case, paleomagnetic stability tests suggest that the ChRM is a primary (or nearly primary) magnetization. Both sedimentary (Summerville and Corral Canyon) and volcanic (Glance Conglomerate and Corral Canyon) rocks are involved, and the ChRM is carried by both magnetite (Corral Canyon and Glance Conglomerate) and hematite (Corral Canyon and Summerville). Before or after structural correction, none of these Middle to Late Jurassic paleomagnetic poles from the southwestern United States (nor any of the VGPs) are located at the high latitudes suggested by the results from New England and the Newark Basin. Thus based on the paleomagnetic poles from the southwestern United States, we propose that the Jurassic North American apparent polar wander path is an age-progressive band at 55°N to 65°N latitude extending from ~110°E longitude at ~172 Ma to ~150°E longitude at ~149 Ma.

Acknowledgments. We thank Steve Vasas and John Buggenhagen for help with the field and laboratory work. The comments of Laurie Brown and an anonymous reviewer were useful for improving the manuscript. This project was funded by National Science Foundation grant EAR 9017382.

REFERENCES

Baars, D. L., et al., Basins of the Rocky Mountain Region, in *The Geology of North America*, vol. D-2, *Sedimentary Cover—North American Craton: U.S.*, edited by L. L. Sloss, pp. 109–220, Geological Society of America, Boulder, Colo., 1988.

Bazard, D. R., and R. F. Butler, Paleomagnetism of the Chinle and Kayenta Formations, New Mexico and Arizona, *J. Geophys. Res.*, *96*, 9847–9871, 1991.

Besse, J., and V. Courtillot, Revised and synthetic apparent polar wander paths of the African, Eurasian, North American and Indian plates, and true polar wander since 200 Ma, *J. Geophys. Res.*, *96*, 4029–4050, 1991.

Bryan, P., and R. G. Gordon, Rotation of the Colorado Plateau: An updated analysis of paleomagnetic data, *Geophys. Res. Lett.*, *17*, 1501–1504, 1990.

Condon, S. M., and A. C. Huffman, Revisions in nomenclature of the Middle Jurassic Wanakah Formation, northwestern New Mexico and northeastern Arizona, *U.S. Geol. Soc. Bull.*, *1633-A*, 1988.

Fisher, R. A., Dispersion on a sphere, *Proc. Roy. Soc. London, Ser. A*, *217*, 295–305, 1953.

Gordon, R. G., A. Cox, and S. O'Hare, Paleomagnetic Euler poles and the apparent polar wander and absolute motion of North America since the Carboniferous, *Tectonics*, *3*, 499–537, 1984.

Halverson, E., A paleomagnetic pole position of Late Jurassic/Early Cretaceous dolerites from Hinlopenstretet, Svalbard, and its tectonic implications, *Earth Planet. Sci. Lett.*, *94*, 398–408, 1989.

Hamilton, W., Plate-tectonic mechanism of Laramide deformation, *Contrib. Geol.*, *19*, 87–92, 1981.

Harland, W. B., R. L. Armstrong, A. V. Cox, L. E. Craig, A. G. Smith, and D. G. Smith, *A Geologic Time Scale, 1989*, Cambridge University Press, New York, 1990.

Heller, F., Paleomagnetism of Upper Jurassic limestones, *J. Geophys.*, *42*, 167–175, 1977.

Imlay, R. W., Jurassic paleobiogeography of the coterminous United States in its continental setting, *U.S. Geol. Surv. Prof. Pap.*, *1062*, 67–99, 1980.

Johnson, R. J. E., R. Van der Voo, and W. Lowrie, Paleomagnetism and late diagenesis of Jurassic carbonates from the Jura mountains, Switzerland and France, *Geol. Soc. Am. Bull.*, *95*, 478–488, 1984.

Kadzialko-Hofmokl, M., J. Kruczyk and M. Westphal, Paleomagnetism of Jurassic sediments from the western border of the Rheingraben, Alsace (France), *J. Geophys.*, *62*, 102–108, 1988.

Kadzialko-Hofmokl, M., and J. Kruczyk, Paleomagnetism of middle-late Jurassic sediments from Poland and implications for the polarity of the geomagnetic field, *Tectonophysics*, *139*, 53–66, 1987.

Kirschvink, J. L., The least-squares line and plane and the analysis of paleomagnetic data: examples from Siberia and Morocco, *Geophys. J. R. Astron. Soc.*, *62*, 699–718, 1980.

Kluth, C. F., R. F. Butler, L. E. Harding, M. Shafiqullah, and P. E. Damon, Paleomagnetism of Late Jurassic rocks in the northern

Canelo Hills, southeastern Arizona, *J. Geophys. Res.*, *87*, 7079–7086, 1982.

Kowalis, B. J., E. H. Christiansen, and A. L. Deino, Age of the Brushy Basin Member of the Morrison Formation, Colorado Plateau, Western USA, *Cretaceous Res.*, *12*, 483–493, 1991.

May, S. R., and R. F. Butler, North American Jurassic apparent polar wander: Implications for plate motion, paleogeography, and Cordilleran tectonics, *J. Geophys. Res.*, *91*, 11,519–11,544, 1986.

May, S. R., R. F. Butler, M. Shafiqullah, and P. E. Damon, Paleomagnetism of Jurassic volcanic rocks in the Patagonia Mountains, southeastern Arizona: Implications for the North American 170 Ma reference pole, *J. Geophys. Res.*, *91*, 11,545–11,555, 1986.

McFadden, P. L., The best estimate of Fisher's precision parameter K, *Geophys. J. R. Astron. Soc.*, *60*, 397–407, 1980.

McElhinny, M. W., and D. L. Jones, Paleomagnetic measurements on some Karroo Dolerites from Rhodesia, *Nature*, *206*, 921–922, 1965.

McFadden, P. L., and M. W. McElhinny, Classification of the reversal test in paleomagnetism, *Geophys. J. Int.*, *103*, 725–729, 1990.

McFadden, P. L., and F. J. Lowes, The discrimination of mean directions drawn from Fisher distributions: *Geophys. J. R. Astron. Soc.*, *67*, 19–33, 1981.

Pipiringos, G. N., and R. B. O'Sullivan, Principal unconformities in Triassic and Jurassic rocks, western interior United States—A preliminary survey, *U.S. Geol. Surv. Prof. Pap.*, *1035–A*, 29 pp., 1978.

Prevot, M., and M. McWilliams, Paleomagnetic correlation of Newark Supergroup volcanics, *Geology*, *17*, 1007–1010, 1989.

Smith, T. E., and H. C. Noltimier, Paleomagnetism of the Newark trend igneous rocks of the north central Appalachians and the opening of the central Atlantic Ocean, *Am. J. Sci.*, *279*, 778–807, 1979.

Steiner, M. B., Magnetic polarity during the Middle Jurassic as recorded in the Summerville and Curtis formations, *Earth Planet. Sci. Lett.*, *38*, 331–345, 1978.

Steiner, M. B., and C. E. Helsley, Jurassic polar movement relative to North America, *J. Geophys. Res.*, *77*, 4981–4993, 1972.

Van Fossen, M. C., and D. V. Kent, High-latitude paleomagnetic poles from Middle Jurassic plutons and moat volcanics in New England and the controversy regarding Jurassic apparent polar wander for North America, *J. Geophys. Res.*, *95*, 17,503–17,516, 1990.

Witte, W. K., and D. V. Kent, A middle Carnian to early Norian (~225 Ma) paleopole from sediments of the Newark Basin, Pennsylvania, *Geol. Soc. Am. Bull.*, *101*, 1118–1126, 1989.

Witte, W. K., and D. V. Kent, The paleomagnetism of red beds and basalts of the Hettangian extrusive zone, Newark Basin, New Jersey, *J. Geophys. Res.*, *95*, 17,533–17,545, 1990.

D. R. Bazard, Department of Geology and Geological Engineering, University of Mississippi, University, MS 38677.

R. F. Butler, Department of Geosciences, University of Arizona, Tucson, AZ 85721.